ELSEVIER

Ceramics International 29 (2003) 355–361

CERAMICS INTERNATIONAL

www.elsevier.com/locate/ceramint

Sintering of silicon carbide II. Effect of boron

Ludoslaw Stobierski*, Agnieszka Gubernat

Department of Advanced Ceramics, Faculty of Materials Engineering and Ceramics, University of Mining and Metallurgy, al. Mickiewicza 30, 30-059 Cracow, Poland

Received 3 May 2002; received in revised form 5 June 2002; accepted 1 July 2002

Abstract

The results of investigations on the role of carbon in SiC sintering, presented in the first part of this paper, indicate that this additive prevents the mass transport mechanisms ineffective in densification. Thereby they suggest that porosity is eliminated due to boron. In order to verify such a hypothesis we measured the kinetics of SiC sintering at constant temperature of 2150 °C. The samples used in this study, contained carbon at a constant concentration of 3 wt.% and boron up to 4 wt.%. It was found that at the carbon concentration of 3 wt.% the optimum addition of boron was 0.2–0.5 wt.%. Although the results of kinetic measurements did not allow for a unanimous identification of the mass transport mechanism, they revealed an unexpectedly high rate of densification. Within 60 s the system reached 0.9 theoretical density. Microstructural observations combined with the results of kinetic measurements suggest that boron activates the sintering process by promoting the formation of a liquid phase, Si–B–C.

Keywords: A. Sintering; D. Silicon carbide; D. Carbon; Boron; Sintering activators

1. Introduction

In order to obtain dense single-phase sintered bodies of silicon carbide it is necessary to activate the SiC powder with small amounts of boron and carbon [1]. The role played by both additives in the sintering process has not been fully clarified so far. As far as carbon is concerned, the experimental data collected for many years indicate that this additive prevents thermal decomposition of SiC and thereby it modifies the kinetics of matter transport. It reduces by itself the rate of some transport processes thought to be ineffective in sintering, such as diffusion in the gas phase or surface diffusion [2–4]. The experimental evidence on the role of boron is not sufficient. However, in view of the fact that carbon acts as an inhibitor of ineffective mass transport mechanisms it might be expected that boron activates the mechanisms which favour densification of SiC. This idea is consistent with the results reported by Lange and Gupta. They suggest that a liquid boron–silicon–carbon phase activates the densification process [5]. However, further more convincing experimental data are necessary in order to confirm this. In the present work the effect of boron concentration on microstructure and isothermal sintering kinetics of SiC was studied.

2. Experimental

The starting material was UF-15 Starck α-SiC powder, phenol-formaldehyde resin Novolak (Organika-Sarzyna) as the carbon source and Fluka (cat. No. 15580) amorphous boron. Powder mixtures in an alcoholic solution of the resin were homogenized in a ball mill, with SiC balls, for 12 h. After evaporation of alcohol they were granulated and compacted. The obtained materials contained boron in the amounts of: 0.00, 0.0125, 0.025, 0.05, 0.10, 0.20, 0.30, 0.40, 0.50, 1.00, 2.00 and 4.00 wt.% and a fixed addition of the resin which after pyrolysis gave carbon concentration of 3.00 wt.%. The samples were pressed in a steel die under a pressure of 150 MPa and then isostatically densified under 300 MPa. Samples for microstructural examination had a thickness of 8 mm and diameter of 20 mm while those for the kinetic studies dimensions were 4 and 12 mm,

* Correspinding author. Tel.: +48-12-617-24-64; fax: +48-12-633-46-30.

0272-8842/02/$22.00
PII: S0272-8842(02)00144-X

respectively. Pore size distribution by mercury porosimetry and density were measured in case of sintering studies. Heating rate of 15 °C/min up to 1200 °C, then 10 °C/min up to 2150 °C, and 60 min at constant temperature were applied. Powder mixtures were also densified by hot pressing in graphite moulds under pressure 25 MPa. The heating rates were the same as given above but annealing at constant temperature of 2150 °C was shortened to 30 min.

Densification degree of the sintered samples was determined on the basis of hydrostatic weighting. Transverse cross-sections of all samples were prepared for microstructural examinations under the scanning electron microscope and some of them were selected for the preparation of thin foils for transmission electron microscopy.

The kinetics of shrinkage under isothermal conditions was measured using the specially designed dilatometer (Fig. 1). The sample holder was made of an isotropic graphite, which coefficient of thermal expansion was of 6.5×10^{-1} 1/K. The instrument allowed us to record the changes of linear dimensions of a sample with accuracy of 1 μm. The dilatometer was equipped with a two-point pyrometric temperature-control system. One of the pyrometers controlled the furnace and enabled maintaining stable temperature in the measurement zone of the dilatometer, the other—inserted through the aperture in the graphite sample holder—was used to measure the temperature of the sintered sample. The procedure of isothermal sintering comprised the following stages: first the measuring zone was heated to the desired temperature (2150 °C), the boat with the sample to be sintered remained in the cooler part of the furnace, where it was heated to 1300 °C. As soon as the temperature conditions inside the furnace became stable, the boat was pushed to the measuring zone within 5 s. The sample reached the temperature of the furnace (2150 °C) within 10 s. This moment was taken as a starting point for recording the contraction on sintering. The measurements of sintering kinetics were made for the all samples but the measurable shrinkage was registered exclusively in the case of samples containing more than 0.05 wt.% of boron.

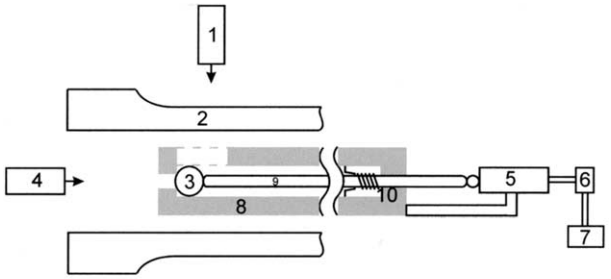

Fig. 1. Scheme of high-temperature dilatometer.

3. Discussion

3.1. Densification degree

Green density of all samples was within the range of 0.61–0.63. Pore size distribution in the samples was monomodal and average pore diameter was 130–140 nm. Both facts indicate geometric similarity of all samples. So differences in the behaviour of different samples during sintering cannot be related to the factor of grain arrangement. The apparent densities of green samples and sintered bodies vs. boron concentration are given in Fig. 2.

Irrespective of the sintering technique (isothermal or polythermal) or hot pressing the tendencies of sintered samples of apparent density corresponding to boron concentration are similar. Apparent densities of the sintered bodies increase with boron concentration within its range of 0.0–0.2 wt.%. The highest values are observed at the boron concentration level of 0.2–0.5 wt.%. Further increase of boron concentration results in decreased apparent densities of the bodies. This is less evident in case of hot-pressing.

3.2. Microstructure of sintered materials

Changes of apparent density influence microstructure of the materials. Along with the increased boron content from 0.0 to 0.1 wt.% sight decrease of porosity is observed. Investigations of microstructure revealed that in these cases sintering occurred in the limited areas—effect of agglomeration is visible (Fig. 3). The grains in these areas have nearly isometric shapes and their

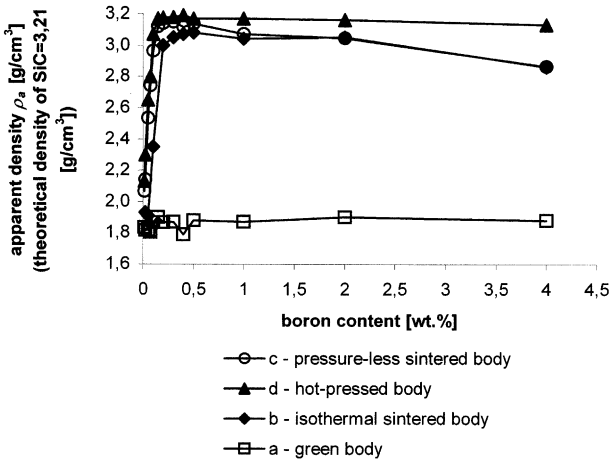

Fig. 2. Apparent density for the following materials: a—green body, b—isothermal sintered body, c—pressure-less (polythermal) sintered body, d—hot-pressed body.

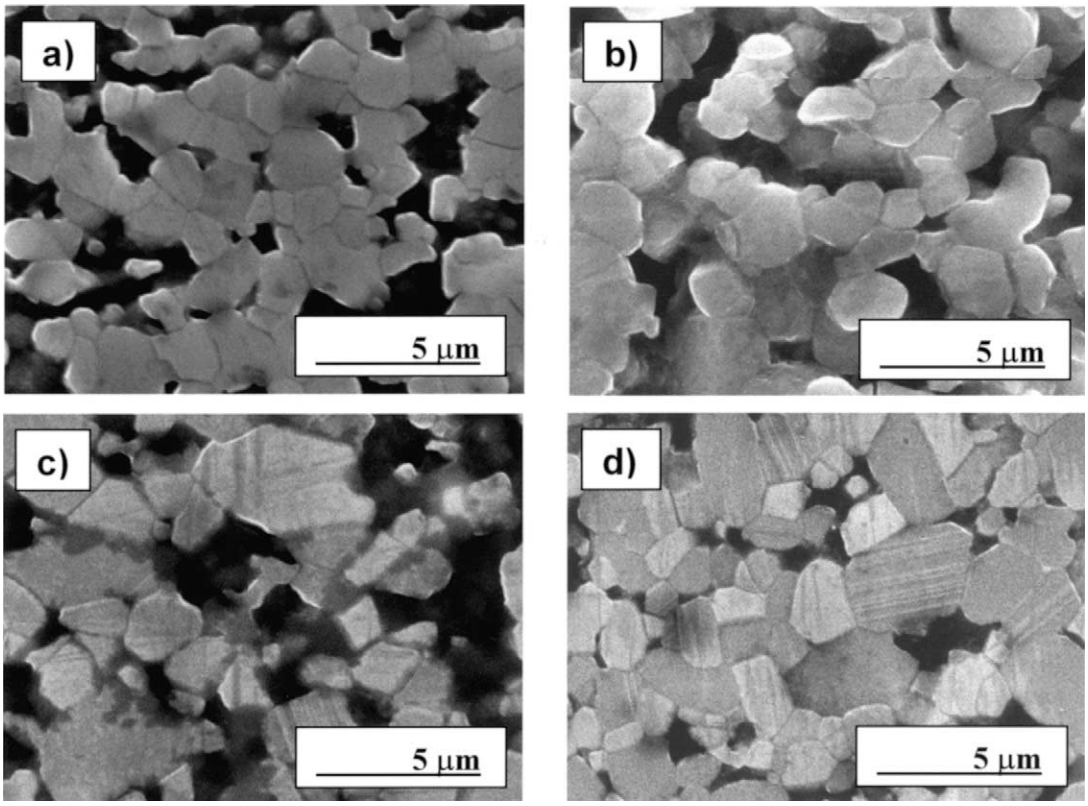

Fig. 3. SEM microstructure of materials containing: a—0.0, b—0.025, c—0.075 and d—0.1 wt.% of boron (all materials containing 3 wt.% of carbon).

average diameters are of the order of 1 μm. There is no evidence of discontinuous grain growth. The microstructures of sintered samples representing the discussed group are shown in Fig. 3.

Microstructure becomes totally different when boron concentration reaches or exceeds 0.2 wt.%. Porosity drops by one order of magnitude. The average grain diameter significantly increases and at boron concentration of 0.50% some symptoms of discontinuous grain growth become evident, manifested by the varying grain-shape ratios (grain length/grain width). The microstructures of samples containing 0.2–0.4 wt.% boron are presented in Fig. 4. At still higher concentrations of boron, exceeding 0.5 wt.%, the discontinuous grain growth becomes distinctly visible, as shown in Fig. 5 for the samples with boron concentrations up to 4.0 wt.%. The tendency to discontinuous and directional grain growth becomes stronger at high boron concentrations. The sintered samples containing at least 1.0 wt.% B are composed of exclusively elongated grains. Along with the sizes and shapes of grains also the shapes of grain boundaries change. While in the previously discussed microstructures, flat grain boundaries were the predominant ones, in the samples containing more than 0.5 wt.% boron there appear curved grain boundaries. The surfaces of grains in the direction

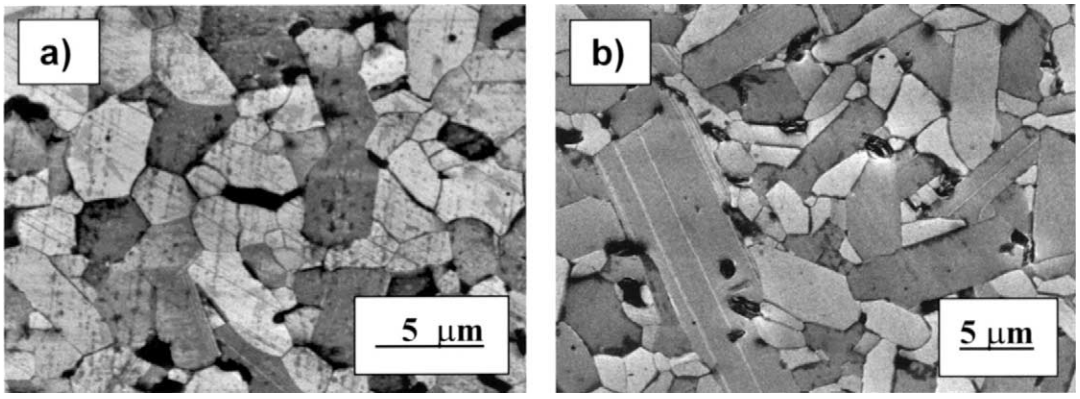

Fig. 4. SEM micrographs of materials containing: a—0.2 and b—0.4 wt.% of boron (both materials containing 3 wt.% of carbon).

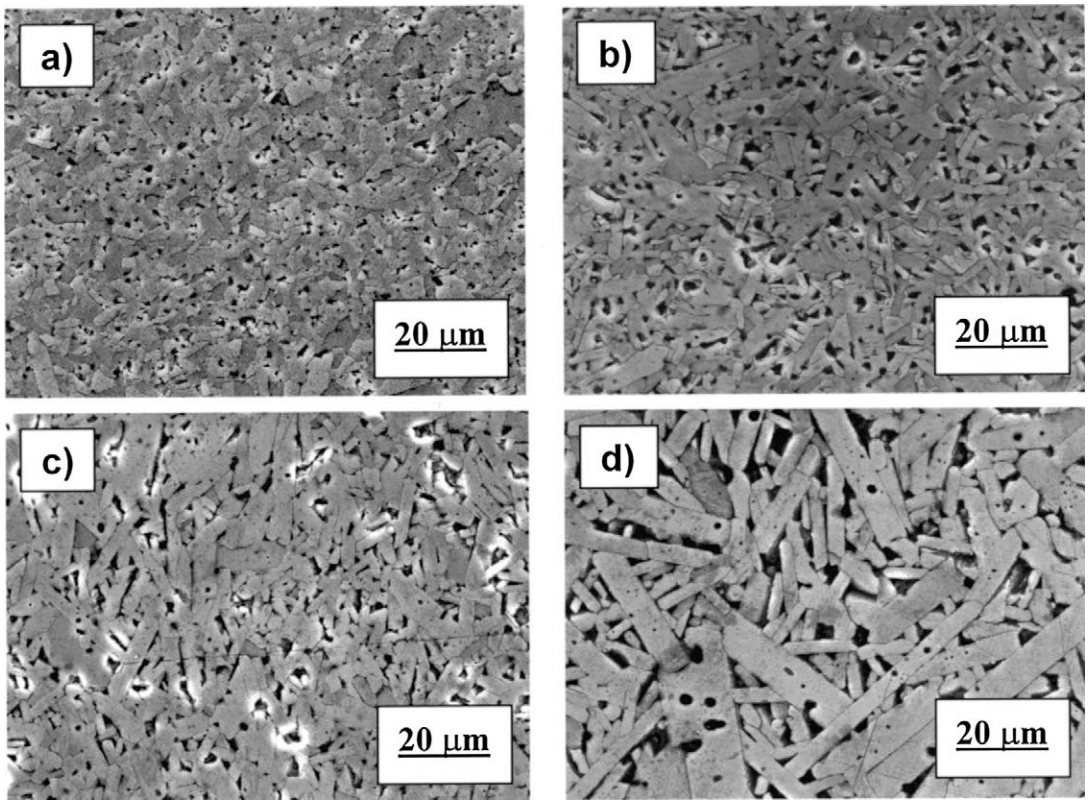

Fig. 5. Tendency to discontinuous and directional grain growth. Sintered bodies containing: (a) 0.5%, (b) 1%, (c) 2% and (d) 4 wt.% of boron (all samples containing 3.0 wt.% of carbon).

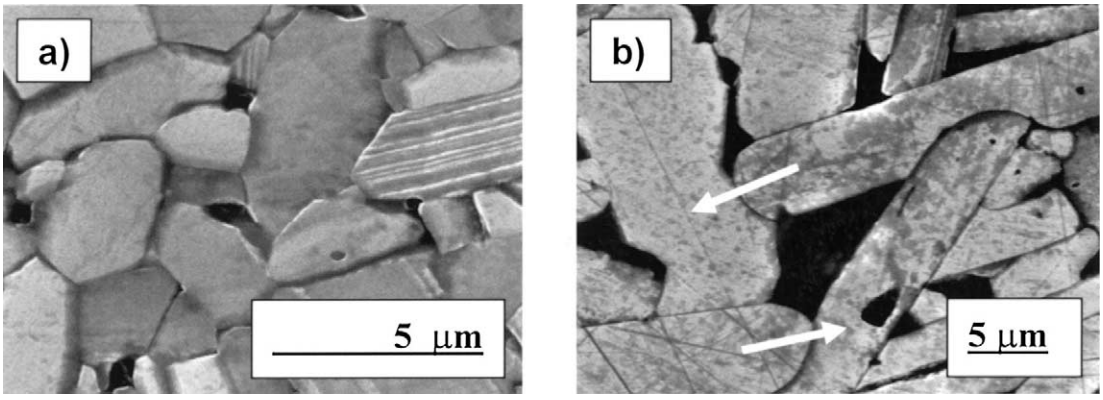

Fig. 6. Hypothetical microstructures of SiC sintered bodies containing: (a) 0.2 wt.% of boron—flat grain boundaries can be seen, (b) 4 wt.% of boron—curved grain boundaries demonstrating of grain growth direction can be seen.

of fast grain growth are convex, as illustrated in Fig. 6. The microscopic images illustrate the features of continuous and discontinuous grain growth and the variations of grain-boundary shapes. The results of microstructural analysis, obtained by means of the Visilog 4 software, including variations of mean equivalent circle grain sections diameter $E(d_2)$ and mean grains sections shape factor $E(F)$, are collected in Table 1.

In addition to the above-described changes of grain shapes and sizes, in the sintered samples containing more than 1.0 wt.% of boron, some spherical occlusions of boron-rich phases are observed in the SiC grains. In

Table 1
The mean equivalent circle grain sections diameter $E(d_2)$ and the mean grain sections shape factor $E(F)$ vs. boron content

Boron (wt.%)	Mean equivalent circle grain sections diameter $E(d_2)$ [μm] (±standard deviation)	Mean grain sections shape factor $E(F)$ (±standard deviation)
0.025	1.190±0.002	1.320±0.001
0.05	1.760±0.003	1.416±0.001
0.15	1.911±0.004	1.438±0.001
0.5	1.876±0.005	1.490±0.001
1.0	2.655±0.009	1.572±0.002
2.0	2.638±0.008	1.581±0.002
4.0	4.537±0.014	1.639±0,002

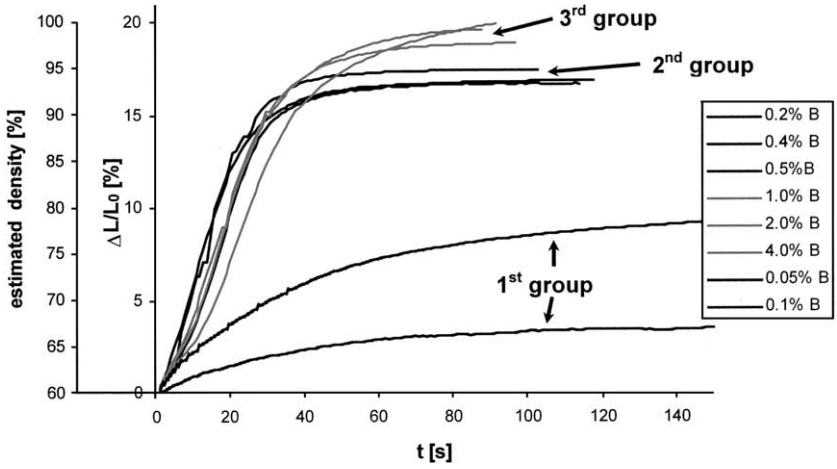

Fig. 7. The dilatometric curves $(\Delta L/L_0) = f(t)$ for isothermal sintered samples containing different addition of boron (from 0.5 to 4 wt.%) and fixed addition of carbon (3.0 wt.%).

the etched specimens only spherical pores are visible since they get dissolved in the fused potassium salts. According to the microscopic observations, in the investigated range of boron concentrations, three groups of materials can be distinguished: materials with boron deficit where sintering is limited and only agglomerates of sintered grains are formed, materials with the optimum concentration of boron, where the sintered grains are almost isometric, and materials with boron excess where discontinuous directional growth of grains takes place.

3.3. Kinetics of isothermal sintering

The dilatometric curves are shown in Fig. 7. Three groups of curves can be distinguished here, similarly as in the case of microstructural observations. In the *first group*, that corresponds to materials with boron concentration less than 0.2 wt.%, shrinkage increases with boron concentration. The curves do not exhibit a "plateau". In the *second group* of curves that corresponds to materials with boron concentration in the range 0.2–0.5 wt.%, after a short time the contraction rate drops to zero. In the *third group*, characteristic of materials with boron content higher than 0.5 wt.%, the initial rate of contraction is close to that observed in the second group but stabilisation of dimensions is not attained—slow creep occurs instead. The curves do not attain a "plateau". On measuring the dimensions of samples it turned out that they get deformed under the load of dilatometric sensor, being as low as 0.5 N.

It is necessary to pay attention to the fact that materials which containing boron from 0.2 to 4.0 wt.% (all samples containing also 3 wt.% of carbon) achieve the density higher than 0.9 of theoretical SiC density in a very short time, close to 60 s. This observation suggests effective role of both activators in the densification process of SiC.

3.4. Mechanism of mass transport

Following the procedure proposed to determine the mechanism of mass transport on the basis of kinetic measurements [6–9], in order to find the exponents in the kinetic equation, the dilatometric curves were plotted in a logarithmic scale. It has been stated that for all the investigated samples the curves after the logarithmic transformation have the form of two straight-line segments. Therefore it might be concluded that two stages with different mass transport mechanisms are involved in SiC sintering. For illustration some curves are shown in Fig. 8. Table 2 collects the values of exponents "*a*" accounting for the theoretically derived mechanisms of mass transport. The values of exponents found for the investigated materials are given in Table 3 [6–9]. By comparing the theoretical and experimental exponents it is not possible to decide which of the mass transport mechanisms dominates at each sintering stage. However it is possible to eliminate the processes which occur at much lower rates, i.e. those for which the theoretical exponents are much smaller than the experimental ones. Unexpectedly high densification rates observed at the first stage of sintering, and corresponding high values of the exponent, suggest that all diffusion mechanisms should be rejected. Thus the mechanisms to be considered include ones involving displacement of grains: in the solid state-rearrangement of grains and in the presence of a liquid phase—viscous flow [8].

The value of exponent "*a*" 0.80 characteristic of materials with boron deficit (up to 0.1 wt.%) cannot be attributed to any of the theoretical mechanisms. It seems to be close to the grain rearrangement. For the remaining materials the slope of first straight-line segment of the plot is higher than 1. Such values are quoted for the viscous flow mechanism when a liquid phase is present [8].

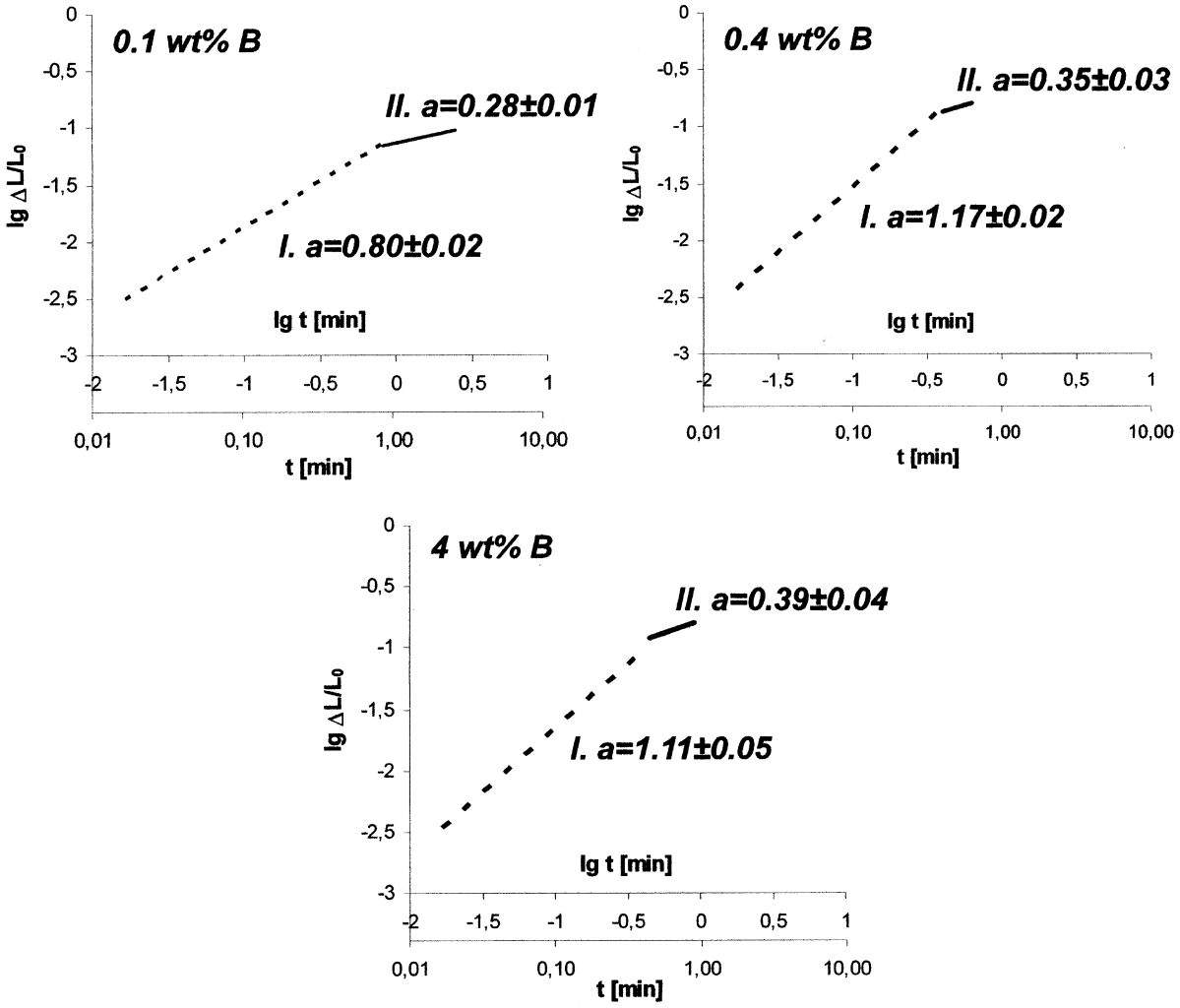

Fig. 8. Curves of linear shrinkage vs. sintering time $(\Delta L/L_0) = f(t)$ were plotted in logarithmic scale for selecting compositions containing different addition of boron and fixed addition of carbon (3.0 wt.%).

Table 2
The values of exponent "a" for different kind of sintering and mass transport mechanisms

Mass transport mechanism	The value of exponent "a"
Solid state sintering	
Rearrangement	1
Bulk diffusion	0.4
Grain boundary diffusion	0.3
Liquid phase sintering	
Viscous flow	>1
Solution-precipitation process (diffusion rate controlling)	0.3
Solution-precipitation process (boundary reaction rate controlling)	0.5

The values of exponent in the second stage of sintering, for all groups of the investigated materials, fall in the range of 0.28–0.39. However, when the deviations from the model system are taken into account and above all the observed grain growth, it becomes rather difficult

Table 3
The calculated "a", estimated density and estimated final density vs. boron content

Boron (wt.%)	Sintering stages	Calculated "a" ±S.D.	Estimated density (%)±5%	Estimated final density (%)±5%
0.05	I	0.80±0.03	65 (50 s)	67%
	II	0.28±0.01	67 (100 s)	
0.1	I	0.80±0.02	75 (50 s)	84%
	II	0.28±0.01	83 (100 s)	
0.2	I	1.19±0.05	92 (25 s)	99%
	II	0.32±0.06	97 (15 s)	
0.4	I	1.17±0.02	90 (20 s)	99%
	II	0.34±0.03	96 (15 s)	
0.5	I	1.23±0.04	93 (20 s)	99%
	II	0.30±0.04	98 (15 s)	
1.0	I	1.18±0.04	90 (30 s)	99%
	II	0.37±0.04	96.5 (20 s)	
2.0	I	1.18±0.05	85 (30 s)	98%
	II	0.37±0.06	96 (30 s)	
4.0	I	1.11±0.05	87 (35 s)	98%
	II	0.39±0.04	95 (30 s)	

to decide about any specific transport mechanism. In Table 3, in addition to experimental values of exponents there are also estimated density degrees and time after which the quoted densification was attained as well as estimated density measured after completion of the sintering process.

4. Discussion

Mictrostructural and kinetic studies permit to distinguish three concentration ranges of boron with in which the trajectory of sintering and the effect of boron are significantly different. The first range is that of very low concentrations, not exceeding the solubility of boron in silicon carbide [10]. The densification degree of the materials increases with boron concentration. It might be supposed that two processes compete, i.e. activation of transport mechanisms and dissolution of boron in SiC.

Boron concentration in the range of 0.2–0.5 wt.% leads to the highest densification of sintered materials without the symptoms of discontinuous growth of the SiC grains. It is therefore the optimum range of activator concentration. Microstructures of the materials within this range of boron concentration are characteristic of sintering in the solid state, i.e. grain boundaries are flat without precipitates, grains are isometric and there is no evidence of discontinuous growth. When the discussed concentration range is exceeded a number of experimental data indicates the presence of a liquid phase. These are grain growth in the direction of convex curvatures and spherical inclusions rich in boron inside the SiC grains. Their shape suggests occlusion of alloy drops. Moreover creep of the material under an extremely small load (0.5 N) of the dilatometric sensor. All the mentioned facts support the hypothesis formulated by Lange and Gupta that sintering of SiC is either a reactive sintering or sintering in presence of a liquid phase [5].

This hypothesis enables explanation of very high densification degrees, of about 0.9, attained in the early stages of the sintering process. Such situation would not be possible by grain rearrangement. The observed behaviour can be explained on the basis of grain-shape accommodation, as assumed by Yoon and Huppmann [11,12]. They conclude that the process of viscous flow accompanied by grain shape accommodation through dissolution and crystallization can lead to densification degrees as high as that.

From the phase diagram given by Kieffer et al. [13] it follows that at the sintering temperature a boron-silicon melt may appear. Its volume fraction depends on the amount of available boron. The composition of this alloy may change in a wide range of boron and silicon concentrations. The alloy can also dissolve carbon. Carbon solubility is, however, limited and its concentration changes may lead to solidification of the melt. At 2150 °C the saturated boron–silicon–carbon liquid phase may have the following molar composition: 0.7 B, 0.2 Si, 0.1 C. Volume fraction of this phase, in the compositional range where the highest densification degrees are observed, is very small. It can be assumed however, that even very small amount of this phase can activate the densification mechanisms. As the amount of boron increases so does the amount of the liquid phase which changes the microstructure and reaction kinetics. The spherical shape of occlusions suggests that the liquid phase was incorporated in the growing SiC grains. The discussed phase is not stable. On lowering the temperature it decomposes. Boron carbide precipitates are formed and silicon becomes incorporated in the surrounding grains structure.

To summarise the above discussion it can be postulated that the role of boron consists in the formation of a liquid phase in the sintered material which enables effective participation of the capillary forces in densification process

References

[1] S. Prochazka, The role of boron and carbon in the sintering of silicon carbide, in: P. Propper (Ed.), Special Ceramics, British Ceramic Research Association, Stoke-on-Trent, 1975, pp. 171–182.
[2] L. Stobierski, A. Gubernat, Sintering aids in silicon carbide densifications, Bulletin of the Polish Academy of Sciences, Technical Sciences 47 (4) (1999) 411–421.
[3] A. Gubernat, The Role of Boron and Carbon in Sintering of Silicon Carbide, PhD thesis, University of Mining and Metallurgy, Cracow, 2001 (in Polish).
[4] J. Lis, R. Pampuch, Sintering, University of Mining and Metallurgy (Ed.), Cracow, 2000, pp. 79–131 (in Polish).
[5] F.F. Lange, T.K. Gupta, Sintering of SiC with boron compounds, J. Am. Ceram. Soc. 59 (11–12) (1976) 537–538.
[6] G.C. Kuczyñski, Self-diffusion in sintering of metallic particles, Trans, AIME 185 (1949) 169–178.
[7] W.D. Kingery, M. Berg, Study of initial stages of sintering solids by viscous flow, evaporation—consideration and self-diffusion, J. Appl. Phys. 26 (10) (1955) 1205–1212.
[8] W.D. Kingery, Densification during sintering in the presence of a liquid phase, I. Theory, J. Appl. Phys. 30 (3) (1959) 301–310.
[9] J. E. Geguzin, Physics of Sintering, Science, Moscow, 1967, pp. 46–98 (in Russian).
[10] P.T.B. Shaffer, Solubility of boron in alpha silicon carbide, Mater. Res. Bull. 5 (1970) 519–522.
[11] D.N. Yoon, W.J. Huppmann, Grain growth and densification during liquid phase sintering of W-Ni, Acta Metall. 27 (1979) 693–698.
[12] D.N. Yoon, W.J. Huppmann, Chemically driven growth of tungsten grains during sintering in liquid nickel, Acta Metall 27 (1979) 973–977.
[13] R. Kieffer, E. Gugel, G. Leimer, P. Ettmayer, Untersuchungen im System Bor-Kohlenstoff-Silicium, Ber, Dt. Keram. Ges. 49 (2) (1972) 41–46.